Chemical Science

ROYAL SOCIETY OF CHEMISTRY

EDGE ARTICLE

View Article Online
View Journal | View Issue

Cite this: *Chem. Sci.*, 2020, **11**, 5447

All publication charges for this article have been paid for by the Royal Society of Chemistry

Received 28th March 2020
Accepted 7th May 2020

DOI: 10.1039/d0sc01796e

rsc.li/chemical-science

Enhancing catalytic alkane hydroxylation by tuning the outer coordination sphere in a heme-containing metal–organic framework†

David Z. Zee [a] and T. David Harris *[ab]

Catalytic heme active sites of enzymes are sequestered by the protein superstructure and are regulated by precisely defined outer coordination spheres. Here, we emulate these protective functions in the porphyrinic metal–organic framework PCN-224 by post-synthetic acetylation and subsequent hydroxylation of the Zr_6 nodes. A suite of physical methods demonstrates that both transformations preserve framework structure, crystallinity, and porosity without modifying the inner coordination spheres of the iron sites. Single-crystal X-ray analyses establish that acetylation replaces the mixture of formate, benzoate, aqua, and terminal hydroxo ligands at the Zr_6 nodes with acetate ligands, and hydroxylation affords nodes with seven-coordinate, hydroxo-terminated Zr^{4+} ions. The chemical influence of these reactions is probed with heme-catalyzed cyclohexane hydroxylation as a model reaction. By virtue of passivated reactive sites at the Zr_6 nodes, the acetylated framework oxidizes cyclohexane with a yield of 68(8)%, 2.6-fold higher than in the hydroxylated framework, and an alcohol/ketone ratio of 5.6(3).

Introduction

Nature widely employs the iron porphyrin, or heme, prosthetic group to catalyze a remarkably diverse range of challenging oxidative transformations, including C–H bond functionalization.[1] These reactions require the heme active site to form highly reactive intermediates,[2] which must be enveloped by the local protein environment in order to function.[3] Without sequestration by the protein superstructure, molecular heme complexes readily condense into oxo-bridged Fe^{III}_2 species.[4] In addition to immobilization provided by the protein, its folding pattern precisely regulates the chemical environment of the heme. For example, structural and molecular dynamics analyses of cytochrome P450, catalase, and peroxidase enzymes suggest excess water is expelled from catalytic sites to control hydrogen-bonding interactions, manage proton delivery, and tune heme redox potentials.[5] Together, these design elements have inspired synthetic chemists to pursue steric protection,[6] second coordination sphere hydrogen-bonding,[7] macromolecular encapsulation,[8] and immobilization[9] strategies in developing structural and functional models of heme enzymes.

Metal–organic frameworks possess a number of traits well-suited to the study of biomimetic heme chemistry. In particular, porphyrinic frameworks rigidly separate metalloporphyrin units with atomic-level precision,[10–15] thus replicating the sequestering role of proteins. Moreover, through judicious selection of pore size, shape, and environment, solution-phase substrates and reagents can readily diffuse into microporous catalysts.[16] Crucially, metal–organic frameworks can often be prepared in single-crystalline form, which enables structural characterization of the first coordination sphere at reactive metal centers with atomic resolution. Indeed, researchers have harnessed this feature to study unusual metal–ligand binding modes[17] and to structurally elucidate intermediates in catalytic,[18] photoinduced,[19] and cooperative[20] reactions. Along these lines, we have recently shown that four-coordinate metalloporphyrins within the Zr-based framework PCN-224 (ref. 13*b*) can support reactive dioxygen[14a,b,d] and carbonyl[14c] complexes that otherwise elude structural characterization.

In the context of framework-based catalysis, precise synthetic control of pore environment is vital because the pores constitute the outer coordination spheres of catalytic metal active sites. For instance, one challenge here is addressing non-periodic defects, such as the replacement of a multitopic structural linker with monotopic ligands that introduce anomalously reactive sites.[21] This linker replacement phenomenon is especially prominent in PCN-224 and related Zr-based

[a]*Department of Chemistry, Northwestern University, 2145 Sheridan Road, Evanston, Illinois 60208, USA*

[b]*Department of Chemistry, University of California, Berkeley, Berkeley, California 94720, USA. E-mail: dharris@berkeley.edu*

† Electronic supplementary information (ESI) available: Experimental details and characterization data for all new compounds; crystallographic data for **1**, **1FeCl**, and **2**; detailed results of catalytic cyclohexane oxidation reactions. CCDC 1992907–1992909. For ESI and crystallographic data in CIF or other electronic format see DOI: 10.1039/d0sc01796e

frameworks,[13,22] where as few as half of the coordination sites at the Zr_6 nodes bind structural linkers. Depending on the synthesis conditions, non-structural ligands in Zr frameworks have been variously identified as Brønsted-acidic[23] pairs of aqua and hydroxo ligands,[13,22] nucleophilic hydroxide counter-anions,[24] or formate.[25] Herein, we report the selective post-synthetic acetylation and subsequent hydroxylation of the Zr_6 nodes in free-base and heme-containing PCN-224. Using cyclohexane hydroxylation as a model reaction, we find that these treatments afford pore environments with contrasting influences on the catalytic activity of the heme centers.

Results and discussion

In the absence of post-synthetic treatments, preparations of PCN-224 (ref. 13*b*,14,15) result in a material best formulated as $(H_2TCPP)_3\{Zr_6O_4(OH)_{4.7}(HCO_2)_{2.3}(C_6H_5CO_2)_3(H_2O)_x\}_2$ (H_2TCPP^{4-} = tetraanion of 5,10,15,20-tetrakis(4-carboxyphenyl) porphyrin, see Fig. S1 and Table S1†), which we refer to as "as-synthesized PCN-224." Here, the incorporation of benzoate and formate ligands stems from the use of benzoic acid as the modulator and decomposition of the solvent dimethylformamide, respectively. Inspired by the wealth of post-synthetic modifications that preserve crystallinity of metal–organic frameworks,[26] in addition to the incorporation of monocarboxylates into the Zr_6 nodes of NU-1000 (ref. 22*b* and *d*) and UiO-66,[25,27] we initially treated as-synthesized PCN-224 with a variety of carboxylic acids in an attempt to passivate the Zr_6 clusters. However, we observed incomplete incorporation of acetate ligands, and both acetic and trifluoroacetic acid led to noticeable dissolution of the framework to give green solutions of H_8TCPP^{2+}. We therefore reasoned that PCN-224 is better suited to electrophilic, non-acidic reagents. In support of this hypothesis, treatment of as-synthesized PCN-224 with acetic anhydride afforded the material $(H_2TCPP)_3\{Zr_6O_4(OH)_4(CH_3CO_2)_6\}_2$, PCN-224′ (**1**, see Fig. 1 and ESI† for synthetic details). Importantly, the ^{1}H NMR spectrum of **1** digested in D_2SO_4/dimethylsulfoxide-d_6 shows no detectable traces of formate or benzoate, suggesting that acetic anhydride exchanges formate and benzoate ligands for acetate (see Fig. S1†). Moreover, the mole ratio of H_2TCPP^{4-} to acetate is near the ideal stoichiometry of 3 : 12, suggesting the terminal aqua and hydroxo ligands are also replaced (see Table S1†). The acetate ligands in **1** carry out the esterification of methanol to form methyl acetate (see Fig. S2†). Thus, treatment of **1** with methanol at 60 °C, followed by soaking in wet acetone, resulted in removal of acetate ligands to afford $(H_2TCPP)_3\{Zr_6O_4(\mu\text{-}OH)_4(OH)_6\}_2$ (**2**, see Fig. 1). The ^{1}H NMR spectrum of digested **2** indicates that ~90% of the acetate ligands are removed (see Fig. S1†) and that methanol is not readily incorporated (see Table S1†). Finally, heating **1** with $FeCl_3$ and 2,6-lutidine in dimethylformamide, followed by treatment with acetic anhydride,‡ affords **1FeCl** (see Fig. 2 and ESI† for experimental details), which in turn can be hydroxylated to afford **2FeCl**.

A suite of physical and spectroscopic methods demonstrates that acetylation and hydroxylation at the Zr_6 nodes are chemically orthogonal to the first coordination sphere of the heme.

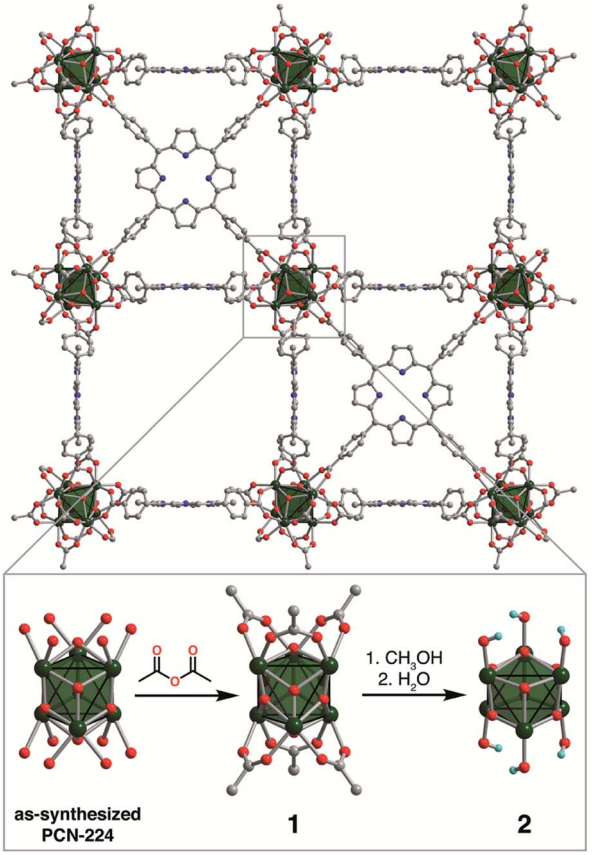

Fig. 1 Treatment of as-synthesized PCN-224, which contains a mixture of formate, benzoate, hydroxo, and aqua ligands, with acetic anhydride affords acetylated six-connected Zr_6 nodes (**1**), as revealed by single-crystal X-ray crystallography. Subsequent treatment of **1** with methanol and water removes the acetate ligands to give Zr_6 nodes with terminal hydroxo ligands (**2**). Green octahedra represent Zr_6 clusters; red, blue, gray, and light blue spheres represent O, N, C, and H atoms, respectively; H atoms, except those of terminal hydroxo ligands, are omitted for clarity. The node structure of as-synthesized PCN-224 is reproduced from ref. 14*a*; the formate and benzoate ligands could not be crystallographically located.

The powder X-ray diffractograms show that bulk crystallinity is retained by ligand substitution at the Zr_6 nodes (see Fig. S3†). UV-vis spectroscopy of **1** and **2** (see Fig. S4†) *versus* **1FeCl** and

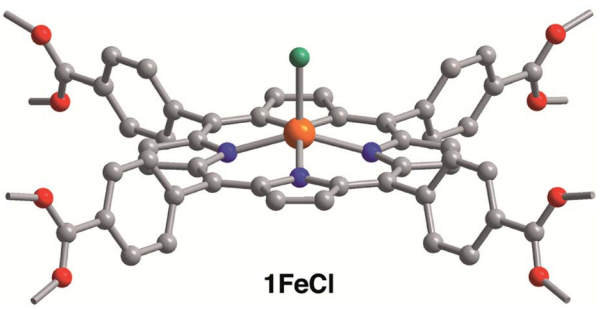

Fig. 2 Crystal structure of the metalloporphyrin unit in **1FeCl**. Orange, teal, red, blue, and gray spheres represent Fe, Cl, O, N, and C atoms, respectively; H atoms are omitted for clarity. Selected interatomic distances (Å): Fe–Cl 2.23(2), Fe–N 2.084(6), Fe···N_4 plane 0.575(8).

2FeCl (see Fig. S5†), in addition to trace metals analysis, indicate that the metalloporphyrins are not demetalated and the chloride ion remains bound to the heme. The zero-field ^{57}Fe Mössbauer spectra for **1FeCl** and **2FeCl** display broad, asymmetric quadrupole doublets characteristic of high-spin, chloro-ligated ferric hemes[28] and are identical to the spectrum for (TPP)FeCl (H_2TPP = 5,10,15,20-tetraphenylporphyrin, see Fig. S6 and Table S2†).

The acetylation and hydroxylation of the Zr_6 nodes were confirmed with single-crystal X-ray analysis. Structures of **1** and **1FeCl** were both solved in the space group $Im\bar{3}m$, with similar unit cell parameters, as previously reported structures of PCN-224 (ref. 13*b*,14,15) (see Table S3† for crystallographic details and Fig. S7, S8† for ellipsoid plots). At the equatorial face of each Zr_6 octahedron, the O atoms refine to two positions of near 50 : 50 occupancy, reflecting the stoichiometry of bridging oxo *versus* hydroxo ligands (see Fig. S10†). In addition, each Zr_6 node coordinates six acetates (see Fig. 1), each either bridging neighboring Zr^{4+} ions or chelating a single Zr^{4+} ion in a κ^2 mode (see Fig. S11†). The X-ray structure of **2** reveals each Zr_6 node to coordinate only six terminal hydroxo ligands, with no additional aqua ligands (see Fig. 1 and S9†), thus establishing seven-coordinate Zr centers in **2**. At 1.910(6) Å, the short Zr–O distance is consistent with Zr–OH bonds (see Table S4†). To our knowledge, this result provides the first structurally characterized example of seven-coordinate Zr within a metal–organic framework, which supports the spectral and density functional theory investigations that suggest rigorous activation of Zr-based frameworks can expose undercoordinated Zr atoms.[22*f*] Finally, the X-ray structure of **1FeCl** shows the expected square pyramidal Fe and confirms that the chloro ligand is not lost upon acetylation (see Fig. 2).

Diffuse reflectance infrared Fourier transform spectroscopy (DRIFTS) supports the assignment of terminal hydroxo ligands in **2** and **2FeCl**. The DRIFTS spectra for **1** and **1FeCl** show the expected μO–H stretches at 3620–3700 cm^{-1} (see Fig. 3; see Fig. S12† for full spectrum), while the DRIFTS spectra for **2** and **2FeCl** show higher-energy peaks between 3720–3800 cm^{-1}. These energies are in good agreement with the bridging and terminal hydroxides of zirconia.[29]

Surface area measurements show that porosity is maintained in these frameworks upon acetylation and subsequent hydroxylation. The N_2 adsorption isotherms for desolvated **1**, **2**, **1FeCl**, and **2FeCl** display uptakes characteristic of microporous adsorbents (see Fig. S12†). Fitting the isotherms to the Brunauer–Emmett–Teller (BET) equation afforded surface areas of 3586(15), 3638(16), 3011(9), and 3204(9) m^2 g^{-1} for **1**, **2**, **1FeCl** and **2FeCl**, respectively (see Fig. S13–S16 and Table S5†). These experimental BET surface areas are in excellent agreement with the N_2-accessible surface areas calculated[30] from their corresponding crystal structures (see Table S6†). Notably, the BET surface areas measured here are higher than the 2400–3000 m^2 g^{-1} of reported PCN-224 frameworks.[13*b*,14–15] The higher gravimetric surface areas may be attributed to the removal of benzoate ligands, thereby decreasing crystal densities of the frameworks, to our solvent exchange and activation procedure

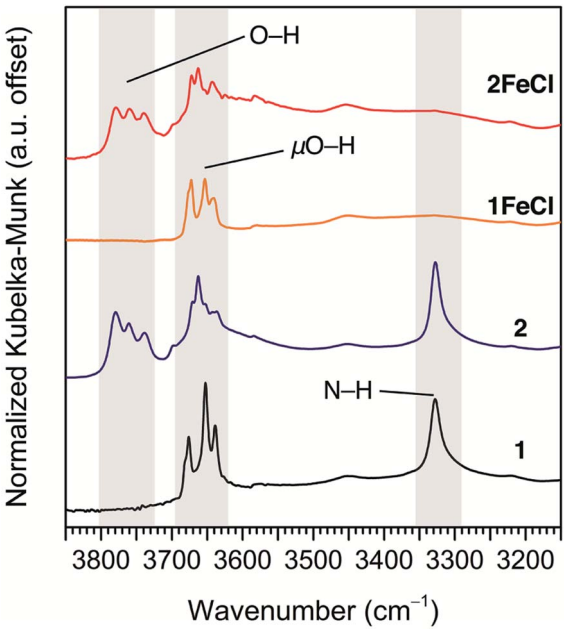

Fig. 3 DRIFTS spectra highlighting the ν(O–H), ν(μO–H), and ν(N–H) modes in **1** (black), **2** (navy), **1FeCl** (orange), and **2FeCl** (red). The absence of porphyrin N–H stretches indicates quantitative iron insertion into **1FeCl** and **2FeCl**. The features between 3720–3800 cm^{-1} are assigned to ν(O–H) modes of terminal hydroxo ligands at the Zr_6 clusters of **2** and **2FeCl**.

(see ESI† for details), or to the improved phase purity afforded by our PCN-224 preparations.

With the Zr_6 coordination environments well-established, we subsequently probed the chemical ramifications of acetylation and hydroxylation using catalytic cyclohexane oxidation as a model reaction. While a number of metalloporphyrin-based frameworks have successfully used olefin epoxidation to demonstrate the accessibility of catalytic metal sites,[31] we eschewed this strategy largely because molecular hemes are already proficient in epoxidation catalysis.[6*b*,32] Furthermore, mounting evidence implicates both metalloporphyrin-oxidant adducts and metalloporphyrin oxo complexes as active intermediates capable of epoxidizing olefins,[33] which could potentially complicate the interpretation of catalytic results. The molecular complex (TPP)FeCl reacts with iodosylbenzene and cyclohexane in a solution of CH_2Cl_2 to produce a mixture of cyclohexanol, cyclohexanone, and chlorocyclohexane in a combined yield of 9(5)%, consistent with previous reports (see Fig. 4 and Table S7†).[6*b*–*d*] In contrast, oxidation yields for **1FeCl** and **2FeCl** are 68(8)% and 26(5)%, respectively. Assuming every Fe atom in the frameworks participates in catalysis, these yields correspond to turnover numbers of 14(2) and 5(1) for **1FeCl** and **2FeCl**, respectively (see Table S7†). The improvement in oxidation yields with **1FeCl** and **2FeCl** *versus* (TPP)FeCl arises from the ability of PCN-224 to afford isolated, catalytically active heme sites, and agrees well with the greater alkane hydroxylation yields observed for sterically encumbered molecular heme complexes.[6*c*,*d*,*f*] On the basis of the oxidation yield of 68(8)%,

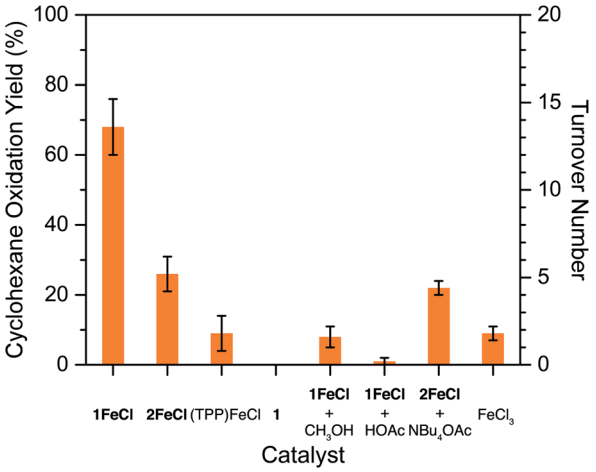

Fig. 4 Cyclohexane oxidation yields with iodosylbenzene. With the acetylated framework **1FeCl** as the catalyst, yields are 2.6-times larger than with the hydroxylated framework **2FeCl**. Error bars reflect one standard deviation ($n = 3$); $OAc^- = CH_3COO^-$.

acetate exchange between **1FeCl** and iodosylbenzene to form (diacetoxyiodo)benzene[34] is likely slow.

While a number of framework-based manganese porphyrins have been shown to oxidize unactivated C–H bonds in alkanes,[10a,31b,35] to our knowledge the present results represent only the third example of such reactions with heme sites.[16c,36] Previously, heme frameworks have been shown to oxidize cyclohexane with *tert*-butylhydroperoxide and *cis*-decalin with 2-*tert*-butylsulfonyliodosylbenzene (^{t}BuSO$_2$PhIO). Among all reported Fe and Mn porphyrin frameworks capable of oxidizing cyclohexane, **1FeCl** ranks fifth-highest based on overall yield, and second-highest among frameworks that use iodosylbenzene as the terminal oxidant (see Table S8†). Notably, the more active Fe and Mn frameworks all favor the formation of cyclohexanone, with alcohol/ketone (A/K) ratios ≤ 0.81. An A/K ratio of one or less implies a radical chain autoxidation mechanism, in which the role of the metal is to generate free radicals.[37] In contrast, **1FeCl** favors the formation of cyclohexanol, with an A/K ratio of 5.6(3) that is consistent with metal-based oxidation.[37] Of note, the selectivity of **2FeCl** for cyclohexanol is even greater (see Table S7†). The lack of over-oxidized cyclohexanone product may be due to the decreased activity of the hydroxylated framework (see below).

Crucially, the cyclohexane oxidation yields of **1FeCl** *versus* **2FeCl** demonstrate that acetylation of the Zr_6 nodes improves the catalytic activity by 2.6-fold (see Fig. 4). Several control experiments suggest that acidic protons within the framework pores impair the oxidative reactivity at the heme centers. For instance, addition of methanol or acetic acid to catalytic reactions with **1FeCl** results in a 9- to 70-fold decrease in cyclohexane oxidation yields (see Fig. 4). Addition of tetrabutylammonium acetate to reactions with **2FeCl** has no significant impact on yields, suggesting that catalysis is enhanced only if reactive proton sources are removed from the Zr_6 nodes, and not improved by acetate ions alone. Control experiments with the free-base framework **1** and $FeCl_3$ confirm that the heme unit is responsible for catalysis (see Fig. 4).

A similar reactivity trend arises when ^{t}BuSO$_2$PhIO,[38] a more soluble iodosylarene reagent, is instead used as the terminal oxidant. Again, oxidation yields are highest with the acetylated framework **1FeCl**, a 30-fold increase relative to the hydroxylated framework **2FeCl**, and a 70-fold increase relative to (TPP)FeCl (see Table S9†). Notably, the yields with ^{t}BuSO$_2$PhIO are significantly lower than with iodosylbenzene. Since ^{t}BuSO$_2$PhIO is more soluble in CH_2Cl_2, it affords higher concentrations of iodosylarene, and thus faster rates of metal-catalyzed disproportionation.[6d,38] Also, ^{t}BuSO$_2$PhIO may be inactivated by the Zr_6 nodes in PCN-224, as the reagent was recently demonstrated to ligate molecular Zr_6 clusters.[34]

Conclusions

The foregoing results demonstrate the facile and quantitative acetylation and hydroxylation of the Zr_6 nodes in free-base and heme PCN-224, with the former reaction giving significant enhancement of C–H bond activation chemistry by virtue of removing labile acidic protons within framework pores. These results outline a path toward isolating and interrogating catalytically competent models of fleeting intermediates in heme enzymes.

Conflicts of interest

There are no conflicts to declare.

Acknowledgements

This work was supported by the U. S. Army Research Office (W911NF-14-1-0168/P00005) and made use of the IMSERC at Northwestern University (NU), which received support from NSF ECCS-1542205, the State of Illinois, and the International Institute for Nanotechnology. The catalysis studies made use of a gas chromatograph purchased by Prof. SonBinh T. Nguyen. Surface area and DRIFTS measurements were performed at the NU REACT Core (DE-FG02-03ER15457). Metals analysis was performed at the NU Quantitative Bio-element Imaging Center. We thank Mr Youwei Shu for experimental assistance.

Notes and references

‡ Additional treatment with acetic anhydride after metalation in dimethylformamide is required to ensure the Zr_6 nodes remain quantitatively acetylated. We found that soaking **1** in neat dimethylformamide at ambient temperature for 12 h replaces ~5% of the acetate ligands with formate. At 100 °C, ~50% of the acetates are replaced.

1 (*a*) M. Sono, M. P. Roach, E. D. Coulter and J. H. Dawson, *Chem. Rev.*, 1996, **96**, 2841–2888; (*b*) *Cytochrome P450: Structure, Mechanism, and Biochemistry*, ed. P. R. Ortiz de Montellano, Springer US, Boston, MA, 3rd edn, 2005; (*c*) T. L. Poulos, *Chem. Rev.*, 2014, **114**, 3919–3962.

2 (*a*) J. T. Groves, *J. Chem. Educ.*, 1985, **62**, 928–931; (*b*) J. Rittle and M. T. Green, *Science*, 2010, **330**, 933–937; (*c*) C. M. Krest,

E. L. Onderko, T. H. Yosca, J. C. Calixto, R. F. Karp, J. Livada, J. Rittle and M. T. Green, *J. Biol. Chem.*, 2013, **288**, 17074–17081; (*d*) X. Huang and J. T. Groves, *Chem. Rev.*, 2018, **118**, 2491–2553; (*e*) M. Guo, T. Corona, K. Ray and W. Nam, *ACS Cent. Sci.*, 2019, **5**, 13–28.

3 (*a*) J. P. Klinman, *Acc. Chem. Res.*, 2007, **40**, 325–333; (*b*) R. L. Shook and A. S. Borovik, *Inorg. Chem.*, 2010, **49**, 3646–3660; (*c*) K. M. Lancaster, in *Molecular Electronic Structures of Transition Metal Complexes I*, ed. D. M. P. Mingos, P. Day and J. P. Dahl, Springer Berlin Heidelberg, Berlin, Heidelberg, 2012, vol. 142, pp. 119–153; (*d*) S. P. de Visser, *Chem.–Eur. J.*, 2020, **26**, 5308–5327.

4 (*a*) A. B. Hoffman, D. M. Collins, V. W. Day, E. B. Fleischer, T. S. Srivastava and J. L. Hoard, *J. Am. Chem. Soc.*, 1972, **94**, 3620–3626; (*b*) D.-H. Chin, G. N. La Mar and A. L. Balch, *J. Am. Chem. Soc.*, 1980, **102**, 4344–4350.

5 (*a*) T. I. Oprea, G. Hummer and A. E. García, *Proc. Natl. Acad. Sci. U. S. A.*, 1997, **94**, 2133–2138; (*b*) P. Jones, *J. Biol. Chem.*, 2001, **276**, 13791–13796; (*c*) K. D. Dubey and S. Shaik, *Acc. Chem. Res.*, 2019, **52**, 389–399.

6 (*a*) J. P. Collman, *Acc. Chem. Res.*, 1977, **10**, 265–272; (*b*) J. T. Groves, R. C. Haushalter, M. Nakamura, T. E. Nemo and B. J. Evans, *J. Am. Chem. Soc.*, 1981, **103**, 2884–2886; (*c*) J. T. Groves and T. E. Nemo, *J. Am. Chem. Soc.*, 1983, **105**, 6243–6248; (*d*) M. J. Nappa and C. A. Tolman, *Inorg. Chem.*, 1985, **24**, 4711–4719; (*e*) B. R. Cook, T. J. Reinert and K. S. Suslick, *J. Am. Chem. Soc.*, 1986, **108**, 7281–7286; (*f*) D. Dolphin, T. G. Traylor and L. Y. Xie, *Acc. Chem. Res.*, 1997, **30**, 251–259; (*g*) W. Liu and J. T. Groves, *Acc. Chem. Res.*, 2015, **48**, 1727–1735.

7 (*a*) G. E. Wuenschell, C. Tetreau, D. Lavalette and C. A. Reed, *J. Am. Chem. Soc.*, 1992, **114**, 3346–3355; (*b*) C. K. Chang, Y. Liang, G. Aviles and S.-M. Peng, *J. Am. Chem. Soc.*, 1995, **117**, 4191–4192; (*c*) C.-Y. Yeh, C. J. Chang and D. G. Nocera, *J. Am. Chem. Soc.*, 2001, **123**, 1513–1514; (*d*) S. A. Cook and A. S. Borovik, *Acc. Chem. Res.*, 2015, **48**, 2407–2414.

8 (*a*) J. T. Groves and R. Neumann, *J. Am. Chem. Soc.*, 1989, **111**, 2900–2909; (*b*) R. Breslow, *Acc. Chem. Res.*, 1995, **28**, 146–153; (*c*) I. C. Reynhout, J. J. L. M. Cornelissen and R. J. M. Nolte, *Acc. Chem. Res.*, 2009, **42**, 681–692.

9 (*a*) J. H. Wang, *J. Am. Chem. Soc.*, 1958, **80**, 3168–3169; (*b*) P. Battioni, E. Cardin, M. Louloudi, B. Schöllhorn, G. A. Spyroulias, D. Mansuy and T. G. Traylor, *Chem. Commun.*, 1996, 2037–2038; (*c*) L. L. Welbes and A. S. Borovik, *Acc. Chem. Res.*, 2005, **38**, 765–774.

10 Selected reviews of porphyrinic metal–organic frameworks: (*a*) K. S. Suslick, P. Bhyrappa, J. H. Chou, M. E. Kosal, S. Nakagaki, D. W. Smithenry and S. R. Wilson, *Acc. Chem. Res.*, 2005, **38**, 283–291; (*b*) M. Zhao, S. Ou and C.-D. Wu, *Acc. Chem. Res.*, 2014, **47**, 1199–1207; (*c*) W.-Y. Gao, M. Chrzanowski and S. Ma, *Chem. Soc. Rev.*, 2014, **43**, 5841–5866; (*d*) Z. Guo and B. Chen, *Dalton Trans.*, 2015, **44**, 14574–14583.

11 (*a*) B. F. Abrahams, B. F. Hoskins and R. Robson, *J. Am. Chem. Soc.*, 1991, **113**, 3606–3607; (*b*) B. F. Abrahams, B. F. Hoskins, D. M. Michail and R. Robson, *Nature*, 1994, **369**, 727–729.

12 A. M. Shultz, O. K. Farha, J. T. Hupp and S. T. Nguyen, *J. Am. Chem. Soc.*, 2009, **131**, 4204–4205.

13 (*a*) D. Feng, Z.-Y. Gu, J.-R. Li, H.-L. Jiang, Z. Wei and H.-C. Zhou, *Angew. Chem., Int. Ed.*, 2012, **51**, 10307–10310; (*b*) D. Feng, W.-C. Chung, Z. Wei, Z.-Y. Gu, H.-L. Jiang, Y.-P. Chen, D. J. Darensbourg and H.-C. Zhou, *J. Am. Chem. Soc.*, 2013, **135**, 17105–17110; (*c*) N. Huang, S. Yuan, H. Drake, X. Yang, J. Pang, J. Qin, J. Li, Y. Zhang, Q. Wang, D. Jiang and H.-C. Zhou, *J. Am. Chem. Soc.*, 2017, **139**, 18590–18597.

14 (*a*) J. S. Anderson, A. T. Gallagher, J. A. Mason and T. D. Harris, *J. Am. Chem. Soc.*, 2014, **136**, 16489–16492; (*b*) A. T. Gallagher, M. L. Kelty, J. G. Park, J. S. Anderson, J. A. Mason, J. P. S. Walsh, S. L. Collins and T. D. Harris, *Inorg. Chem. Front.*, 2016, **3**, 536–540; (*c*) A. T. Gallagher, C. D. Malliakas and T. D. Harris, *Inorg. Chem.*, 2017, **56**, 4654–4661; (*d*) A. T. Gallagher, J. Y. Lee, V. Kathiresan, J. S. Anderson, B. M. Hoffman and T. D. Harris, *Chem. Sci.*, 2018, **9**, 1596–1603.

15 (*a*) J. M. Zadrozny, A. T. Gallagher, T. D. Harris and D. E. Freedman, *J. Am. Chem. Soc.*, 2017, **139**, 7089–7094; (*b*) C.-J. Yu, M. D. Krzyaniak, M. S. Fataftah, M. R. Wasielewski and D. E. Freedman, *Chem. Sci.*, 2019, **10**, 1702–1708.

16 (*a*) F. Song, C. Wang, J. M. Falkowski, L. Ma and W. Lin, *J. Am. Chem. Soc.*, 2010, **132**, 15390–15398; (*b*) D. J. Xiao, J. Oktawiec, P. J. Milner and J. R. Long, *J. Am. Chem. Soc.*, 2016, **138**, 14371–14379; (*c*) A. D. Cardenal, H. J. Park, C. J. Chalker, K. G. Ortiz and D. C. Powers, *Chem. Commun.*, 2017, **53**, 7377–7380; (*d*) C.-H. Wang, A. Das, W.-Y. Gao and D. C. Powers, *Angew. Chem., Int. Ed.*, 2018, **57**, 3676–3681; (*e*) A. W. Stubbs, L. Braglia, E. Borfecchia, R. J. Meyer, Y. Román- Leshkov, C. Lamberti and M. Dincă, *ACS Catal.*, 2018, **8**, 596–601; (*f*) W.-Y. Gao, A. D. Cardenal, C.-H. Wang and D. C. Powers, *Chem.–Eur. J.*, 2019, **25**, 3465–3476.

17 (*a*) T. Sawano, Z. Lin, D. Boures, B. An, C. Wang and W. Lin, *J. Am. Chem. Soc.*, 2016, **138**, 9783–9786; (*b*) M. I. Gonzalez, J. A. Mason, E. D. Bloch, S. J. Teat, K. J. Gagnon, G. Y. Morrison, W. L. Queen and J. R. Long, *Chem. Sci.*, 2017, **8**, 4387–4398; (*c*) Z. Niu, X. Cui, T. Pham, P. C. Lan, H. Xing, K. A. Forrest, L. Wojtas, B. Space and S. Ma, *Angew. Chem., Int. Ed.*, 2019, **58**, 10138–10141.

18 (*a*) K. Ikemoto, Y. Inokuma, K. Rissanen and M. Fujita, *J. Am. Chem. Soc.*, 2014, **136**, 6892–6895; (*b*) W. M. Bloch, A. Burgun, C. J. Coghlan, R. Lee, M. L. Coote, C. J. Doonan and C. J. Sumby, *Nat. Chem.*, 2014, **6**, 906–912; (*c*) A. Burgun, C. J. Coghlan, D. M. Huang, W. Chen, S. Horike, S. Kitagawa, J. F. Alvino, G. F. Metha, C. J. Sumby and C. J. Doonan, *Angew. Chem., Int. Ed.*, 2017, **56**, 8412–8416; (*d*) M. T. Huxley, A. Burgun, H. Ghodrati, C. J. Coghlan, A. Lemieux, N. R. Champness, D. M. Huang, C. J. Doonan and C. J. Sumby, *J. Am. Chem. Soc.*, 2018, **140**, 6416–6425; (*e*) R. J. Young, M. T. Huxley, E. Pardo,

N. R. Champness, C. J. Sumby and C. J. Doonan, *Chem. Sci.*, 2020, **11**, 4031–4050.

19 A. J. Blake, N. R. Champness, T. L. Easun, D. R. Allan, H. Nowell, M. W. George, J. Jia and X.-Z. Sun, *Nat. Chem.*, 2010, **2**, 688–694.

20 (*a*) R. L. Siegelman, T. M. McDonald, M. I. Gonzalez, J. D. Martell, P. J. Milner, J. A. Mason, A. H. Berger, A. S. Bhown and J. R. Long, *J. Am. Chem. Soc.*, 2017, **139**, 10526–10538; (*b*) P. J. Milner, R. L. Siegelman, A. C. Forse, M. I. Gonzalez, T. Runčevski, J. D. Martell, J. A. Reimer and J. R. Long, *J. Am. Chem. Soc.*, 2017, **139**, 13541–13553; (*c*) C. M. McGuirk, R. L. Siegelman, W. S. Drisdell, T. Runčevski, P. J. Milner, J. Oktawiec, L. F. Wan, G. M. Su, H. Z. H. Jiang, D. A. Reed, M. I. Gonzalez, D. Prendergast and J. R. Long, *Nat. Commun.*, 2018, **9**, 5133.

21 (*a*) M. Taddei, *Coord. Chem. Rev.*, 2017, **343**, 1–24; (*b*) S. Dissegna, K. Epp, W. R. Heinz, G. Kieslich and R. A. Fischer, *Adv. Mater.*, 2018, **30**, 1704501; (*c*) D. Yang and B. C. Gates, *ACS Catal.*, 2019, **9**, 1779–1798.

22 (*a*) J. E. Mondloch, W. Bury, D. Fairen-Jimenez, S. Kwon, E. J. DeMarco, M. H. Weston, A. A. Sarjeant, S. T. Nguyen, P. C. Stair, R. Q. Snurr, O. K. Farha and J. T. Hupp, *J. Am. Chem. Soc.*, 2013, **135**, 10294–10297; (*b*) P. Deria, J. E. Mondloch, E. Tylianakis, P. Ghosh, W. Bury, R. Q. Snurr, J. T. Hupp and O. K. Farha, *J. Am. Chem. Soc.*, 2013, **135**, 16801–16804; (*c*) N. Planas, J. E. Mondloch, S. Tussupbayev, J. Borycz, L. Gagliardi, J. T. Hupp, O. K. Farha and C. J. Cramer, *J. Phys. Chem. Lett.*, 2014, **5**, 3716–3723; (*d*) P. Deria, W. Bury, J. T. Hupp and O. K. Farha, *Chem. Commun.*, 2014, **50**, 1965–1968; (*e*) S. Yuan, Y.-P. Chen, J. Qin, W. Lu, X. Wang, Q. Zhang, M. Bosch, T.-F. Liu, X. Lian and H.-C. Zhou, *Angew. Chem., Int. Ed.*, 2015, **54**, 14696–14700; (*f*) D. Yang, V. Bernales, T. Islamoglu, O. K. Farha, J. T. Hupp, C. J. Cramer, L. Gagliardi and B. C. Gates, *J. Am. Chem. Soc.*, 2016, **138**, 15189–15196.

23 (*a*) J. Jiang and O. M. Yaghi, *Chem. Rev.*, 2015, **115**, 6966–6997; (*b*) R. C. Klet, Y. Liu, T. C. Wang, J. T. Hupp and O. K. Farha, *J. Mater. Chem. A*, 2016, **4**, 1479–1485; (*c*) S. Ling and B. Slater, *Chem. Sci.*, 2016, **7**, 4706–4712.

24 C. A. Trickett, K. J. Gagnon, S. Lee, F. Gándara, H.-B. Bürgi and O. M. Yaghi, *Angew. Chem., Int. Ed.*, 2015, **54**, 11162–11167.

25 D. Yang, M. A. Ortuño, V. Bernales, C. J. Cramer, L. Gagliardi and B. C. Gates, *J. Am. Chem. Soc.*, 2018, **140**, 3751–3759.

26 (*a*) K. K. Tanabe and S. M. Cohen, *Chem. Soc. Rev.*, 2011, **40**, 498–519; (*b*) S. M. Cohen, *Chem. Rev.*, 2012, **112**, 970–1000; (*c*) J. D. Evans, C. J. Sumby and C. J. Doonan, *Chem. Soc. Rev.*, 2014, **43**, 5933–5951; (*d*) S. M. Cohen, *J. Am. Chem. Soc.*, 2017, **139**, 2855–2863.

27 R. Wei, C. A. Gaggioli, G. Li, T. Islamoglu, Z. Zhang, P. Yu, O. K. Farha, C. J. Cramer, L. Gagliardi, D. Yang and B. C. Gates, *Chem. Mater.*, 2019, **31**, 1655–1663.

28 J. R. Sams and T. B. Tsin, in *The Porphyrins*, ed. D. Dolphin, Academic Press, New York, NY, 1st edn, 1979, ch. 9, vol. 4, pp. 425–478.

29 (*a*) F. Ouyang, J. N. Kondo, K.-i. Maruya and K. Domen, *J. Phys. Chem. B*, 1997, **101**, 4867–4869; (*b*) K. T. Jung and A. T. Bell, *J. Catal.*, 2001, **204**, 339–347.

30 D. Ongari, P. G. Boyd, S. Barthel, M. Witman, M. Haranczyk and B. Smit, *Langmuir*, 2017, **33**, 14529–14538.

31 Examples of olefin epoxidation by Fe porphyrin metal–organic frameworks: (*a*) Z. Zhang, L. Zhang, L. Wojtas, M. Eddaoudi and M. J. Zaworotko, *J. Am. Chem. Soc.*, 2012, **134**, 928–933; (*b*) C. Zou, T. Zhang, M.-H. Xie, L. Yan, G.-Q. Kong, X.-L. Yang, A. Ma and C.-D. Wu, *Inorg. Chem.*, 2013, **52**, 3620–3626.

32 J. T. Groves and T. E. Nemo, *J. Am. Chem. Soc.*, 1983, **105**, 5786–5791.

33 (*a*) W. Nam, M. H. Lim, H. J. Lee and C. Kim, *J. Am. Chem. Soc.*, 2000, **122**, 6641–6647; (*b*) W. J. Song, Y. J. Sun, S. K. Choi and W. Nam, *Chem.–Eur. J.*, 2006, **12**, 130–137; (*c*) M. Guo, H. Dong, J. Li, B. Cheng, Y.-q. Huang, Y.-q. Feng and A. Lei, *Nat. Commun.*, 2012, **3**, 1190; (*d*) M. Guo, Y.-M. Lee, M. S. Seo, Y.-J. Kwon, X.-X. Li, T. Ohta, W.-S. Kim, R. Sarangi, S. Fukuzumi and W. Nam, *Inorg. Chem.*, 2018, **57**, 10232–10240.

34 A. D. Cardenal, A. Maity, W.-Y. Gao, R. Ashirov, S.-M. Hyun and D. C. Powers, *Inorg. Chem.*, 2019, **58**, 10543–10553.

35 (*a*) M. H. Alkordi, Y. Liu, R. W. Larsen, J. F. Eubank and M. Eddaoudi, *J. Am. Chem. Soc.*, 2008, **130**, 12639–12641; (*b*) O. K. Farha, A. M. Shultz, A. A. Sarjeant, S. T. Nguyen and J. T. Hupp, *J. Am. Chem. Soc.*, 2011, **133**, 5652–5655; (*c*) M.-H. Xie, X.-L. Yang, Y. He, J. Zhang, B. Chen and C.-D. Wu, *Chem.–Eur. J.*, 2013, **19**, 14316–14321; (*d*) W. Zhang, P. Jiang, Y. Wang, J. Zhang, J. Zheng and P. Zhang, *Chem. Eng. J.*, 2014, **257**, 28–35.

36 D. Feng, H.-L. Jiang, Y.-P. Chen, Z.-Y. Gu, Z. Wei and H.-C. Zhou, *Inorg. Chem.*, 2013, **52**, 12661–12667.

37 (*a*) M. W. Grinstaff, M. G. Hill, J. A. Labinger and H. B. Gray, *Science*, 1994, **264**, 1311–1313; (*b*) J. Kim, R. G. Harrison, C. Kim and L. Que, *J. Am. Chem. Soc.*, 1996, **118**, 4373–4379; (*c*) A. Gunay and K. H. Theopold, *Chem. Rev.*, 2010, **110**, 1060–1081.

38 D. Macikenas, E. Skrzypczak-Jankun and J. D. Protasiewicz, *J. Am. Chem. Soc.*, 1999, **121**, 7164–7165.

